Associated with a strong resonance created in the structure around 1.4 GHz, it allows to obtain a large bandwidth. Although the coupling strips "s" reach to separate the operation in the two bands, all the parameters are important to have more freedom degrees for the optimization of the structure because the difficulty is here to obtain a good compromise in the two bands. The lower plate, in spite of its relative small dimensions when compared with the frequency in the lower frequency, is, however, a very useful parameter for the optimization.

5. CONCLUSION

The presented antenna is made up of two square stacked metallic plates on a small ground plane. Two U slots are designed in the upper plate which is both connected to the ground plane and the lower patch, thanks to two couples of wires. The working principle is based on the stacked monopolar wire patch, monopole loaded, and filtering principles. The presented configuration allows to obtain a single resonance in the GSM and multiple resonance in the DCS-PCS and UMTS bands. The dimensions of the different parameters and particularly U-slots and wires allow to enhance the coupling between the resonances and then the adjustment of the different frequencies and bandwidths. This radiating element is also a very low-cost, low-profile, small dimension, and wide frequency bandwidth dual-band antenna, showing a high quality of dipolar radiation pattern type and gain.

REFERENCES

1. E. Lee, P.S. Hall, and P. Gardner, Compact dual-band dual-polarisation microstrip patch antenna, Electron Lett 35 (1999), 1034–1036.
2. C. Delaveaud, P. Leveque, and B. Jecko, New kind of microstrip antenna: The monopolar wire-patch antenna, Electron Lett 24 (1992), 2075–2076.
3. L. Zaïd, G. Kossiavas, J.Y. Dauvignac, J. Cazajous, and A. Papiernik, Dual frequency and broad-band antennas with stacked quarter wavelength elements, IEEE Trans Antennas Propag 47 (1999), 654–660.
4. L. Zaïd and R. Staraj, Broadband low profile wire-patch antenna, Microwave Opt Technol Lett 32 (2002), 323–324.
5. R.B. Waterhouse, J.T. Rowley, and K.H. Joyner, Stacked shorted patch, Electron Lett 34 (1998), 612–614.
6. L. Zaïd and R. Staraj, Miniature circular GSM wire-patch antenna on small ground plane, Electron Lett 38 (2002),153–154

UNIPLANAR COUPLED-FED PRINTED PIFA FOR WWAN/WLAN OPERATION IN THE MOBILE PHONE

Cheng-Tse Lee and Kin-Lu Wong
Department of Electrical Engineering, National Sun Yat-Sen University, Kaohsiung 80424, Taiwan; Corresponding author: wongkl@ema.ee.nsysu.edu.tw

Received 20 August 2008

ABSTRACT: *A coupled-fed printed planar inverted-F antenna (PIFA) with a compact uniplanar structure for easy implementation in the mobile phone for WWAN/WLAN operation is presented. The printed PIFA occupies a small area of 10×60 mm^2 and provides two wide operating bands (the lower and upper bands) at about 900 and 2000 MHz for covering GSM850/900/DCS/PCS/UMTS/WLAN six-band operation. The printed PIFA is formed by two coupled-fed PIFAs of different sizes, a longer radiating/coupling portion and a shorter radiating/coupling portion. Owing to the use of the coupling feed, both of the two portions can generate dual-resonance excitation, with the longer portion providing a wide lower band for GSM850/900 operation and the shorter portion providing a wide upper band for DCS/PCS/UMTS/WLAN operation. In addition, the lower and upper bands of the printed PIFA can generally be controlled separately by the longer and shorter portions, making it easy for fine tuning of the desired operating bands in practical applications.* © 2009 Wiley Periodicals, Inc. Microwave Opt Technol Lett 51: 1250–1257, 2009; Published online in Wiley InterScience (www.interscience.wiley.com). DOI 10.1002/mop.24298

Key words: *internal mobile phone antennas; printed PIFA; coupled-fed PIFA; WWAN operation; WLAN operation*

1. INTRODUCTION

Recently, it has been demonstrated that by applying a printed coupling feed to the internal mobile phone antenna such as the planar inverted-F antennas (PIFAs), dual-resonance excitation in the 900 MHz band for bandwidth enhancement or one-eighth wavelength mode excitation at about 900 MHz for antenna size reduction can be obtained [1, 2]. This printed coupling-feed technique requires no increase in the antenna volume and introduces no additional ohmic loss, which are advantageous over the traditional bandwidth-enhancement techniques of adding additional resonators to the antenna's radiating portion [3-6] or adding an external matching network on the system circuit board of the mobile phone [7-10]. However, it is noted that the coupling-feed design studied in [1, 2] is required to be printed on two sides of a dielectric substrate, which makes the substrate thickness and permittivity strongly controlling the contributed capacitance of the coupling feed to the input impedance of the PIFA. This makes the coupling-feed design sensitive to the parameters of the dielectric substrate, and careful alignment of the coupling-feed metal pattern on two sides of the substrate is required.

In this article, we present a promising wideband design of the PIFA with a coplanar coupling feed in the mobile phone. The printed PIFA has a uniplanar metal pattern occupying a compact area and is suitable to be directly printed on the system circuit board of the mobile phone, which makes it easy to fabricate at low cost for practical applications. In addition, the printed PIFA is formed by two separate PIFAs of different sizes, a longer radiating/coupling portion and a shorter radiating/coupling portion. The longer and shorter portions can provide two dual-resonant operating bands for the antenna's lower and upper bands to cover GSM850/900 (824–894/890–960 MHz) and DCS/PCS/UMTS/WLAN (1710–1880/1850–1990/1920–2170/2400–2484 MHz), respectively, in the mobile phone [11]. That is, the five major operating bands for WWAN (wireless wide area network) operation and the 2.4 GHz band for WLAN (wireless local area network) operation are covered, providing WWAN/WLAN dual-network operation for mobile phone applications. Further, the antenna's lower and upper bands can generally be controlled separately by the longer and shorter portions in the proposed PIFA, allowing it easy to fine tune the desired operating bands in practical applications. Antenna geometry and its design considerations are described in this study. The proposed printed PIFA is also fabricated and tested, and the obtained results are presented and discussed. The specific absorption rate (SAR) values of the coupled-fed printed PIFA are also analyzed.

2. PROPOSED UNIPLANAR COUPLED-FED PRINTED PIFA

Figure 1(a) shows the geometry of the uniplanar coupled-fed printed PIFA for WWAN/WLAN operation. The metal pattern of the printed PIFA occupying an area of 10×60 mm^2 only, and its detailed dimensions are shown in Figure 1(b). The uniplanar PIFA

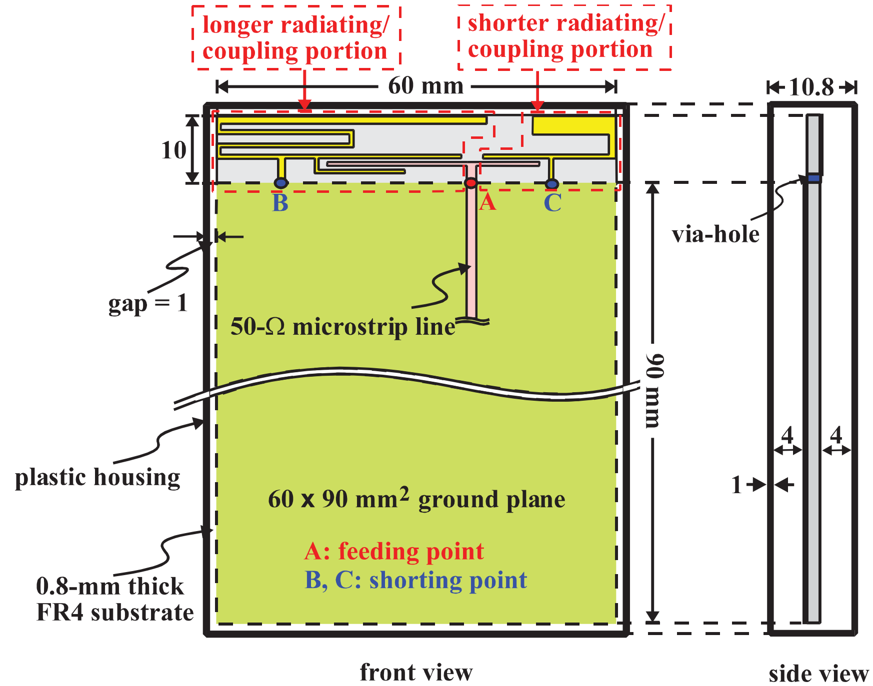

(a)

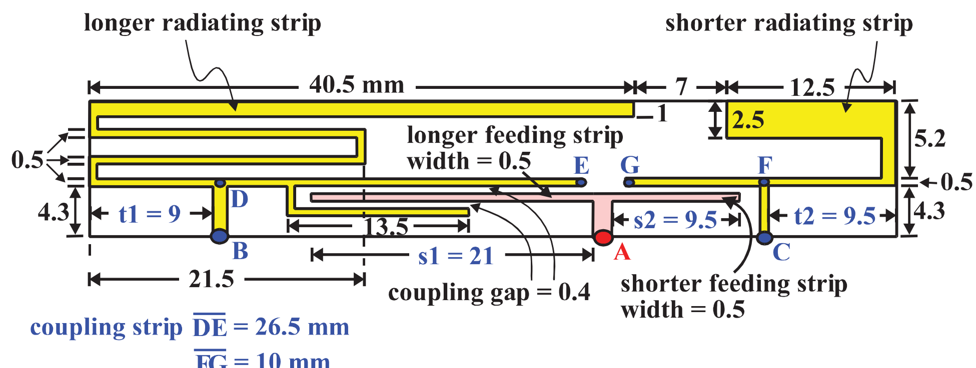

(b)

Figure 1 (a) Geometry of the uniplanar coupled-fed printed PIFA for WWAN/WLAN operation in the mobile phone. (b) Detailed dimensions of the printed PIFA. [Color figure can be viewed in the online issue, which is available at www.interscience.wiley.com]

is printed on the top no-ground region of the system circuit board of length 100 mm and width 60 mm, which is a promising size for the general smart phones or PDA phones [12-14]. In this study, the 0.8-mm thick FR4 substrate of relative permittivity 4.4 and loss tangent 0.0245 is used as the system circuit board, and a system ground plane of 90 $\times$ 60 mm^2 is printed on the back side of the FR4 substrate. The studied antenna is also enclosed by a 1-mm thick plastic housing whose relative permittivity is 3.0 and conductivity is 0.02 S/m. As seen from the side view in the figure, the outer thickness of the plastic housing is selected to be 10.8 mm only, which is attractive for thin mobile phone applications [15, 16]; in this case, the printed PIFA and the ground plane are both spaced the same distance of 4 mm to the inner surface of the plastic housing.

The proposed PIFA mainly consists of a longer radiating/coupling portion and a shorter radiating/coupling portion. The longer and shorter portions are coupled-fed by the T-shaped feeding strip having a longer feeding strip of length (s_1) 21 mm and a

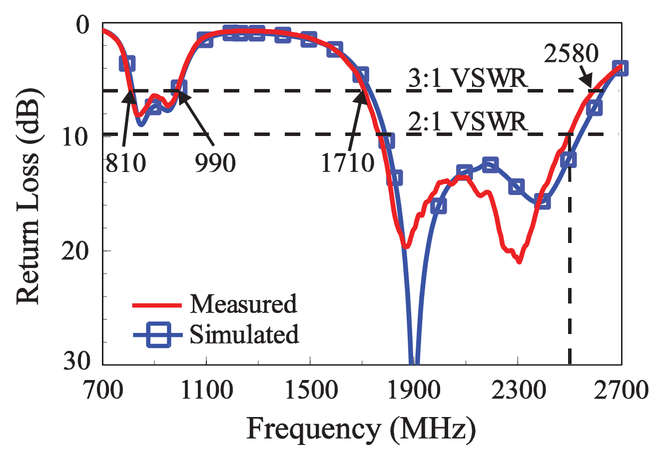

Figure 2 Measured and simulated return loss for the proposed PIFA. [Color figure can be viewed in the online issue, which is available at www.interscience.wiley.com]

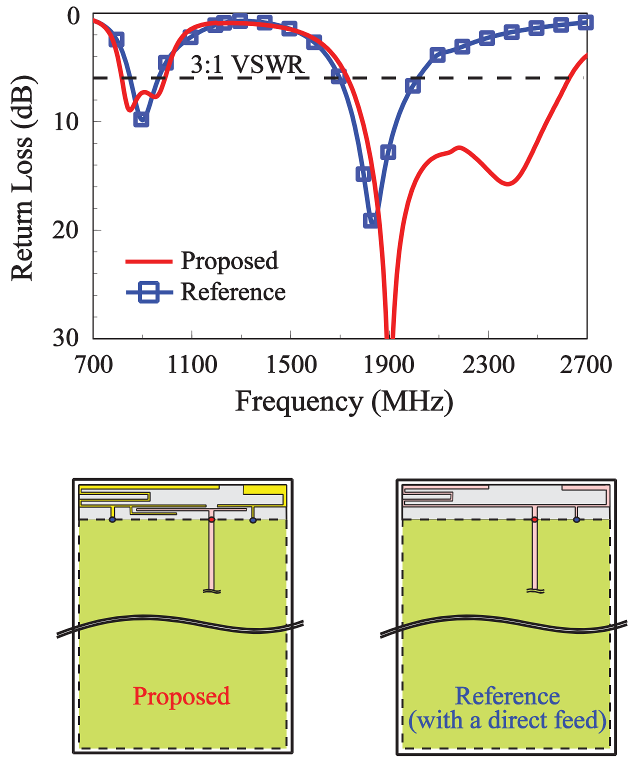

(a)

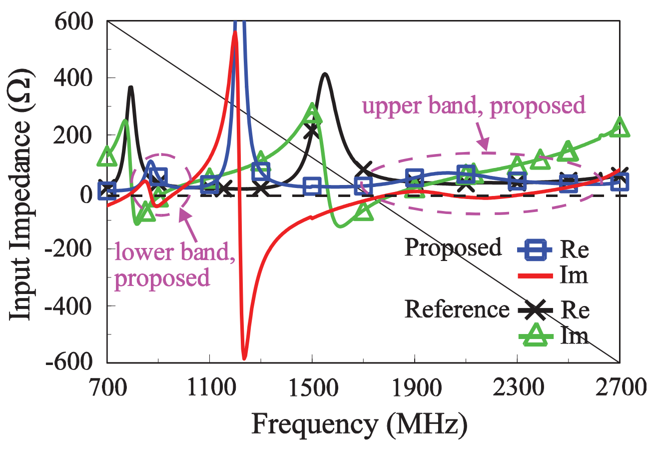

(b)

Figure 3 Comparison of the simulated (a) return loss and (b) input impedance of the proposed PIFA and the reference PIFA (corresponding conventional PIFA with a direct feed). [Color figure can be viewed in the online issue, which is available at www.interscience.wiley.com]

shorter feeding strip of length (s_2) 9.5 mm. In the longer radiating/coupling portion, there are a longer radiating strip of length close to one-quarter wavelength at 900 MHz, a branch-line coupling strip enclosing the longer feeding strip in the T-shaped feeding strip, and a shorting strip $\overline{BD}$ at location (t_1) 9 mm to the left side edge of the antenna. By adjusting the length s_1 and location t_1, dual-resonance excitation can be achieved for the quarter-wavelength resonant mode at about 900 MHz controlled by the longer radiating strip. This dual-resonance mode has a widened bandwidth to cover GSM850/900 operation. Detailed results of the length s_1 and location t_1 on controlling the impedance matching of the antenna's lower band around 900 MHz will be discussed in Figure 5 in Section 3. Also note that all the coupling gaps between the feeding strip and the coupling strip are fixed as 0.4 mm in the design, and the use of the branch-line coupling strip, compared with the use of the coupling strip $\overline{DE}$ only, can result in a much larger contributed capacitance to the antenna's input impedance to achieve a dual-resonance excitation. If the branch-line coupling strip is not used (that is, only the coupling strip $\overline{DE}$ is present), a much longer length s_1 will be required to achieve the same coupling effect as that of using the branch-line coupling strip.

In the shorter radiating/coupling portion, it mainly comprises a shorter radiating strip of length close to one-quarter wavelength at 2000 MHz, a coupling strip $\overline{FG}$ of length 10 mm facing the shorter coupling strip (length s_2 = 9.5 mm) in the T-shaped feeding strip, and a shorting strip $\overline{CF}$ at location (t_2) 9.5 mm to the right side edge of the antenna. For achieving dual-resonance excitation for the antenna's upper band, a simple coupling strip $\overline{FG}$ is sufficient. In the proposed design, the obtained bandwidth of the quarter-wavelength mode at about 2000 MHz is large enough to cover DCS/PCS/UMTS/WLAN operation. Detailed results of adjusting the length s_2 and location t_2 on controlling the impedance matching for the antenna's upper band around 2000 MHz will be discussed in Figure 6.

Note that for testing the proposed printed PIFA, a 50-Ω microstrip line is printed on the system circuit board and connected at point A (the feeding point) to the T-shaped feeding strip of the PIFA. Also, the open-end portion of the shorter radiating strip is widened to have a width of 2.5 mm, which can lead to more uniform excited surface current distributions at around the open end and is also helpful in improving the impedance matching of the antenna [17].

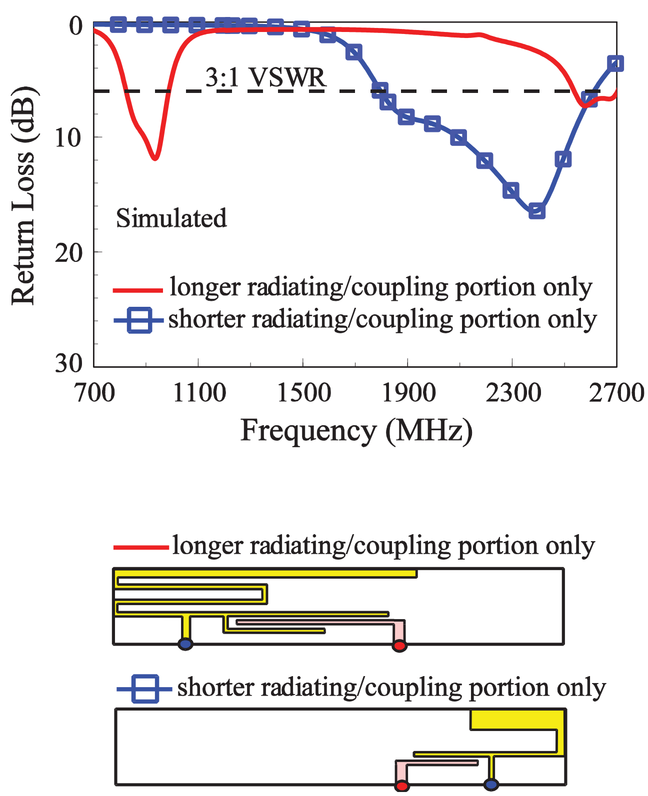

Figure 4 Simulated return loss of the cases with the longer radiating/coupling portion only and the shorter radiating/coupling portion only. [Color figure can be viewed in the online issue, which is available at www.interscience.wiley.com]

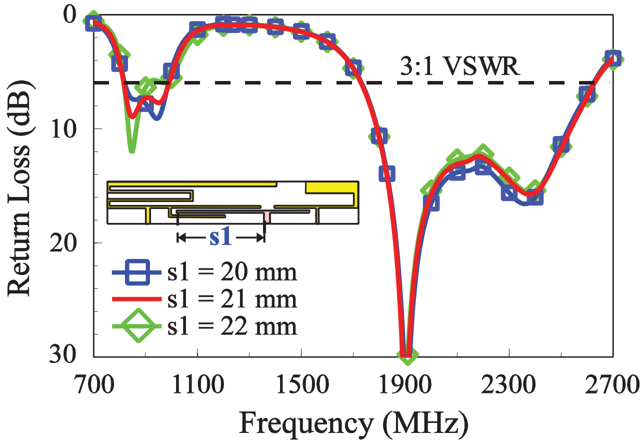

(a)

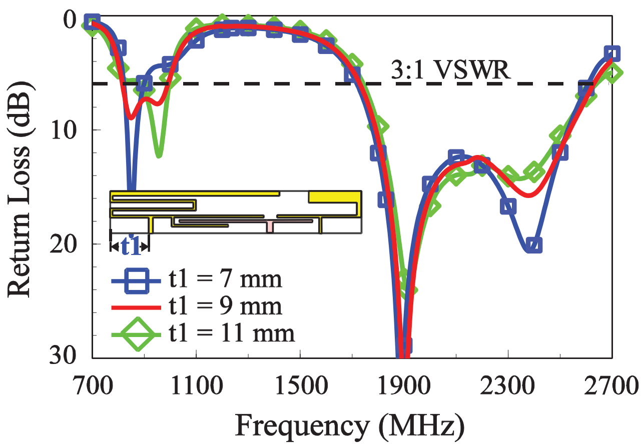

(b)

Figure 5 Simulated return loss as a function of (a) the feeding-strip length s_1 and (b) the shorting-strip location t_1 for the longer radiating/coupling portion. [Color figure can be viewed in the online issue, which is available at www.interscience.wiley.com]

3. RESULTS AND DISCUSSION

The printed PIFA with dimensions shown in Figure 1 was fabricated and tested. Figure 2 shows the measured and simulated return loss of the fabricated prototype. The simulated results are obtained using Ansoft HFSS [18], and good agreement between the simulated results and measured data is observed. Dual-resonance excitation for both the lower and upper bands is seen. For the lower band, the measured bandwidth with the generally accepted 3:1 VSWR definition for the internal mobile phone antenna, is as large as 180 MHz (810–990 MHz), allowing the antenna to easily cover GSM850/900 operation. For the upper band, the measured bandwidth reaches 870 MHz (1710–2580 MHz), also easily cover DCS/PCS/UMTS/WLAN operation. Note that for WLAN operation in the 2.4 GHz band, the measured return loss is better than 2:1 VSWR, acceptable for practical WLAN applications.

Figure 3 shows the comparison of the simulated return loss and input impedance of the proposed PIFA and the reference PIFA (corresponding conventional PIFA with a direct feed). From the simulated return loss shown in Figure 3(a), no dual-resonance excitation is seen for both the lower and upper bands of the reference PIFA; the lower band can cover GSM900 (890–960 MHz) only, whereas the upper band can cover DCS/PCS (1710–1990 MHz). The obtained bandwidths for the reference PIFA are hence much smaller than those of the proposed PIFA. Figure 3(b) shows the real part (Re) and imaginary part (Im) of the simulated input impedance of the proposed and printed PIFAs. It can be seen that owing to the use of the coupling feed in the proposed PIFA, the input impedance level for the excited quarter-wavelength mode at around 900 MHz is greatly decreased when compared with that for the reference PIFA. This makes it possible for the occurrence of the dual-resonance excitation for the desired lower band at 900 MHz. Over the desired upper band, it is seen that the imaginary part of the input impedance is close to zero and the real part varies slightly around 50 Ω for the proposed PIFA. This also leads to the occurrence of dual-resonance excitation for the desired upper band seen in Figure 3(a). A much widened bandwidth is hence obtained for the proposed PIFA to easily cover DSC/PCS/UMTS/WLAN operation.

Figure 4 shows the simulated return loss of the cases with the longer radiating/coupling portion only and the shorter radiating/coupling portion only. From the results, it is clearly seen that the lower band and the upper band of the proposed PIFA are mainly controlled by the longer portion and the shorter portion, respectively. This also indicates that the desired lower and upper bands can generally be controlled separately by the longer and shorter portions, respectively.

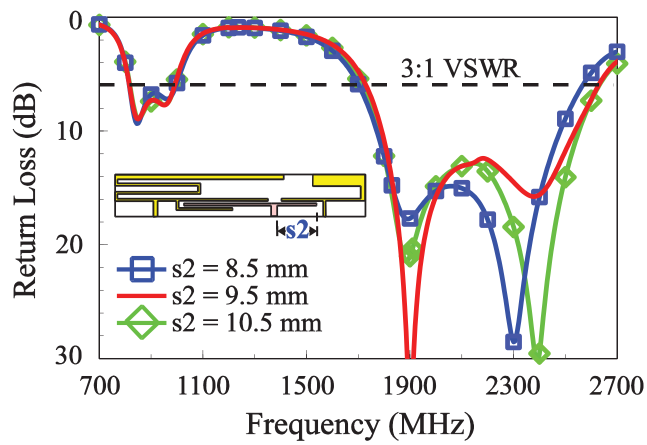

(a)

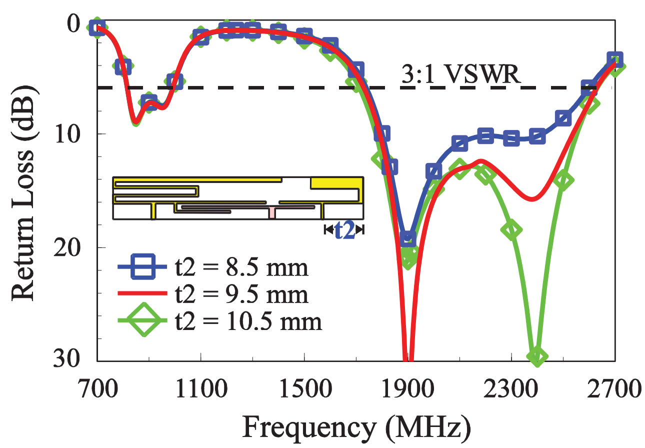

(b)

Figure 6 Simulated return loss as a function of (a) the feeding-strip length s_2 and (b) the shorting-strip location t_2 for the shorter radiating/coupling portion. [Color figure can be viewed in the online issue, which is available at www.interscience.wiley.com]

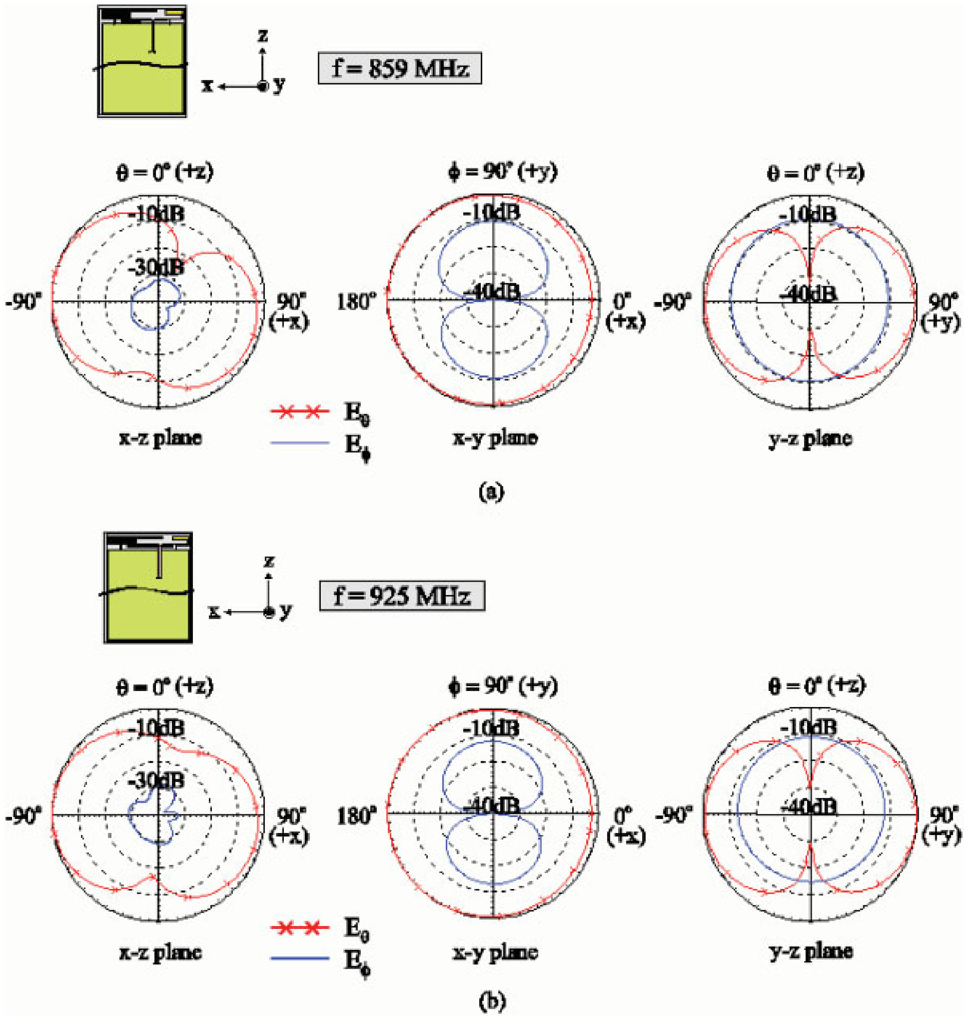

Figure 7 Measured radiation patterns at (a) 859 MHz and (b) 925 MHz for the proposed PIFA. [Color figure can be viewed in the online issue, which is available at www.interscience.wiley.com]

3.1. Parametric Study of the Proposed PIFA

Figure 5 shows the simulated return loss as a function of the feeding-strip length s_1 and the shorting-strip location t_1 for the longer radiating/coupling portion. In Figure 5(a), results for the length s_1 varied from 20 to 22 mm are presented, and other dimensions are the same as given in Figure 1. Large effects on the lower band at about 900 MHz are seen, and however, the upper band is generally not affected. In Figure 5(b), results for the location t_1 varied from 7 to 11 mm are presented; other dimensions are also fixed as given in Figure 1. Similarly, large effects on the lower band are seen, and very small effects on the upper band are also observed. This behavior also confirms that the antenna's lower band can be effectively controlled by the longer radiating/coupling portion in the proposed PIFA; in addition, the antenna's upper band can remain almost unchanged when the parameters of the longer portion are fine adjusted.

Figure 6 shows the simulated return loss as a function of the feeding-strip length s_2 and the shorting-strip location t_2 for the shorter radiating/coupling portion. Results for the length s_2 varied from 8.5 to 10.5 mm are presented in Figure 6(a), whereas those for the location t_2 varied from 8.5 to 10.5 mm are shown in Figure 6(b). Other dimensions in Figures 6(a) and 6(b) are fixed as given in Figure 1. Very small effects on the antenna's lower band are seen for both cases. Over the upper band, relatively small effects on the first resonance at about 1900 MHz are observed. Some large variations on the impedance matching of the second resonance at around 2400 MHz are seen, although the obtained bandwidths of the upper band are about the same. The results also indicate that the shorter portion is dominant on controlling the antenna's upper band, and very small effects on the antenna's lower band can be obtained when the parameters of the shorter portion are fine adjusted.

3.2. Radiation Characteristics of the Proposed PIFA

Figures 7(a) and 7(b) plots the measured radiation patterns at 859 and 925 MHz (central frequencies of GSM850 and GSM900) for the proposed PIFA. Very similar monopole-like radiation patterns are seen for the two frequencies, and good omnidirectional radiation at the azimuth plane (*x-y* plane) is obtained. Figures 8 and 9 show the measured radiation patterns at 1795, 1920, 2045, and 2442 MHz (central frequencies of DCS, PCS, UMTS, and WLAN). More variations in the radiation patterns are seen. This is mainly owing to the increased groundplane length in term of the operating wavelength, which makes the excited surface currents in the ground plane vary more rapidly for frequencies over the upper band than that over the lower band. These measured radiation patterns generally

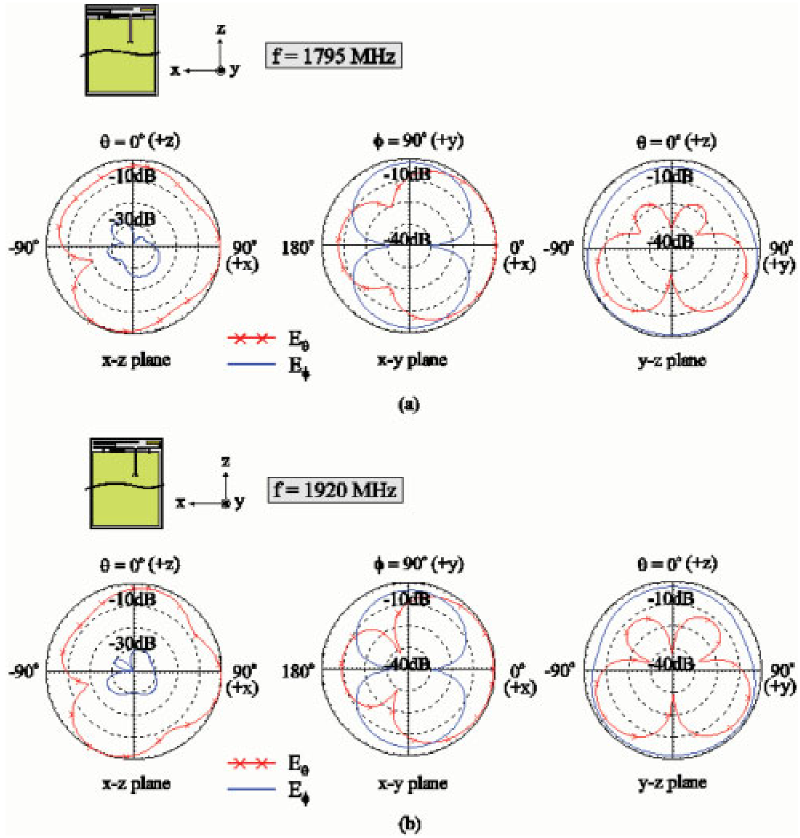

Figure 8 Measured radiation patterns at (a) 1795 MHz and (b) 1920 MHz for the proposed PIFA. [Color figure can be viewed in the online issue, which is available at www.interscience.wiley.com]

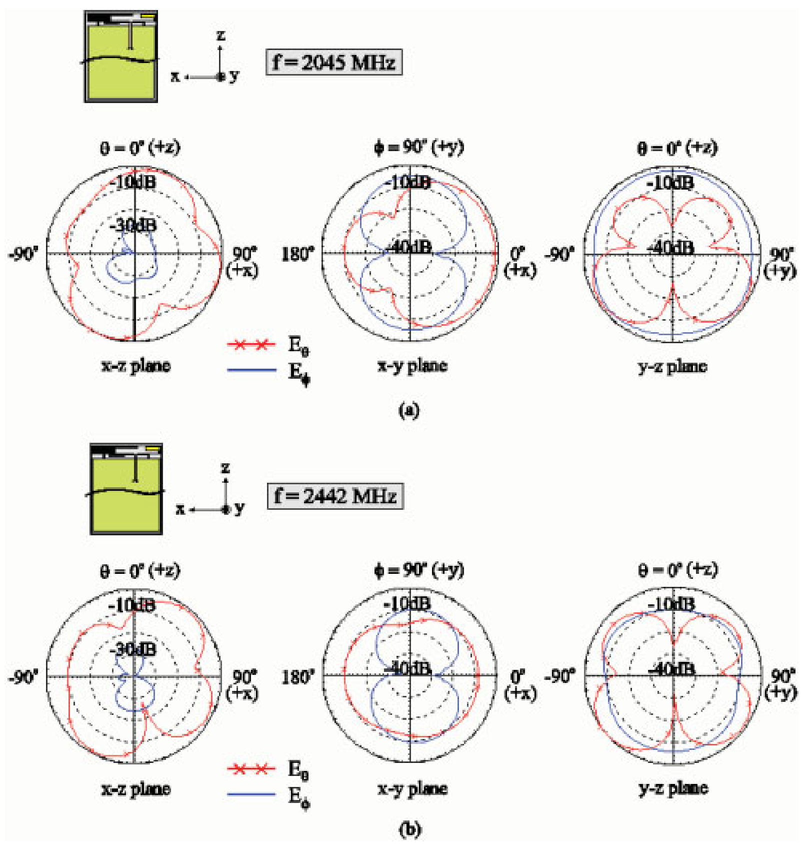

Figure 9 Measured radiation patterns at (a) 2045 MHz and (b) 2442 MHz for the proposed PIFA. [Color figure can be viewed in the online issue, which is available at www.interscience.wiley.com]

show no special distinctions compared with the conventional PIFAs for application in the mobile phone.

Figure 10 shows the measured antenna gain and simulated radiation efficiency for the proposed PIFA. As seen in Figure 10(a), the antenna gain over the GSM850/900 band varies from about −0.1 to 0.9 dBi, and the radiation efficiency is larger than 50%. For the DCS/PCS/UMTS band [see Fig. 10(b)], the antenna gain varies from about 0.8 to 3.5 dBi, and the radiation efficiency is about 57–90%. For the WLAN band, the antenna gain varies from 3.0 to 3.6 dBi, and the radiation efficiency is about 76–84%.

3.3. SAR Analysis of the Proposed PIFA

The SAR values of the proposed PIFA for WWAN operation are analyzed using SEMCAD simulation software [19, 20]. Figure 11 shows the simulation model with the proposed PIFA enclosed by the plastic housing shown in Figure 1 attached onto the phantom ear. Two cases of the PIFA placed at the top position and bottom position are studied. For the top position, the PIFA is at the top edge of the system ground plane; while for the bottom position, the mobile phone is rotated by 180° such that the PIFA is at the bottom edge of the system ground plane. The distance between the metal pattern of the PIFA and the right phantom cheek is 5 mm. For the GSM850/900 band, the SAR is tested using 24 dBm (2 W continuous power in 1/8 time slot); while for the DCS/PCS/UMTS band, the SAR is tested using 21 dBm (1 W continuous power in 1/8 time slot).

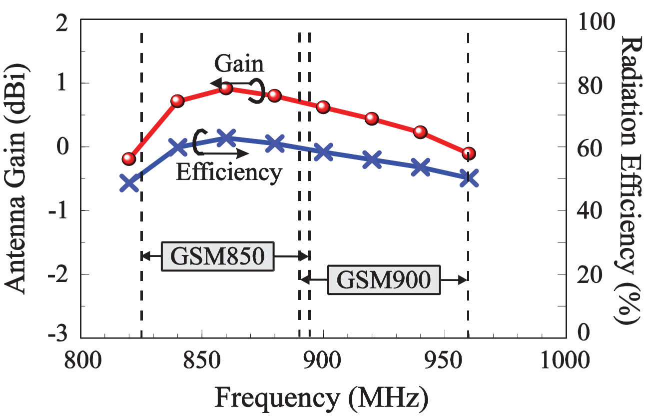

(a)

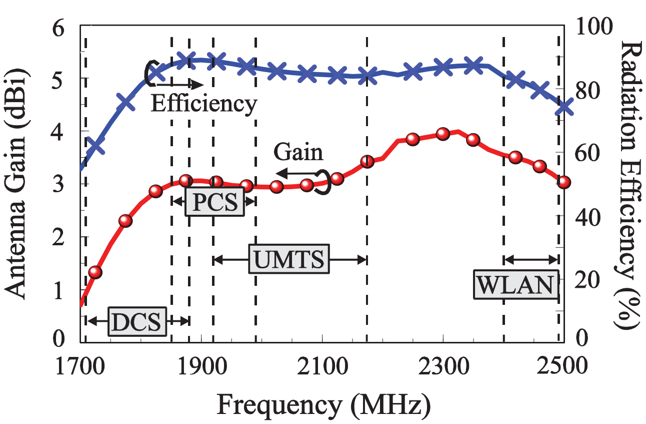

(b)

Figure 10 Measured maximum antenna gain and simulated radiation efficiency for the proposed PIFA: (a) GSM850/900 band; (b) DCS/PCS/UMTS/WLAN band. [Color figure can be viewed in the online issue, which is available at www.interscience.wiley.com]

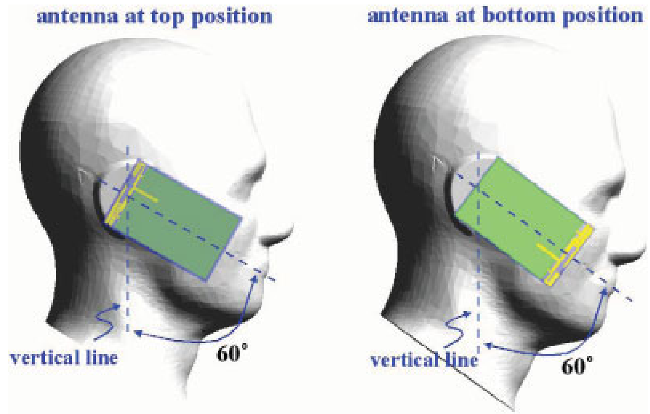

Figure 11 Simulation model (SEMCAD [19]) with the proposed PIFA placed near the phantom ear for two cases of the PIFA at the top position and bottom position. [Color figure can be viewed in the online issue, which is available at www.interscience.wiley.com]

For the top and bottom positions, the obtained 1-g and 10-g average SAR values are listed in Table 1. The SAR decrease between the top and bottom positions is also shown. It is seen that a large decrease in the SAR values (about 1.95–2.81 dB for the GSM850/900 band and about 3.13–4.67 dB for the DCS/PCS/UMTS band) can be obtained by placing the proposed PIFA at the bottom position, compared with that at the top position. This provides a useful design method for the proposed PIFA to achieve decreased SAR values for practical applications. As for the smaller SAR decrease at the lower band than at the upper band for the proposed PIFA placed between the top and bottom positions, it is largely because the system ground plane of the mobile phone usually plays a more dominant role in the radiation of the PIFA for GSM850/900 operation than for DCS/PCS/UMTS operation [21].

4. CONCLUSION

An internal coupled-fed printed PIFA with a uniplanar structure capable of WWAN/WLAN operation in the mobile phone has been proposed and tested. The proposed PIFA occupying a small area of 10 × 60 mm^2 can be easily fabricated at low cost on the system circuit board of the mobile phone. The proposed PIFA can be decomposed into a longer radiating/coupling portion and a shorter radiating/coupling portion. Owing to the use of the coupling feed, each portion can provide a dual-resonance quarter-wavelength mode to achieve a much widened operating band; the longer one generates a wide lower band for covering GSM850/900 operation, whereas the shorter one generates a wide upper band for covering DCS/PCS/UMTS/WLAN operation. That is, a six-band operation for WWAN/WLAN operation has been achieved for the proposed PIFA. Good radiation characteristics for frequencies over the operating bands have also been obtained. The SAR values of the proposed PIFA placed at the top and bottom positions of the mobile phone have also been analyzed. Results indicate that it is promising for the proposed PIFA to be placed at the bottom position of the mobile phone to achieve decreased SAR values for practical applications.

TABLE 1 Simulated SAR (Obtained From SEMCAD [19]) for the Antenna Placed at the Top and Bottom Positions of the Mobile Phone with the Presence of the User's Head

			Antenna at the top position		
Frequency (MHz)	859	925	1795	1920	2045
1-g SAR (*W*/kg)	2.10	2.12	1.73	1.76	1.68
10-g SAR (*W*/kg)	1.42	1.44	0.87	0.84	0.76
			Antenna at the bottom position		
Frequency (MHz)	859	925	1795	1920	2045
1-g SAR (*W*/kg)	1.10	1.25	0.59	0.68	0.72
10-g SAR (*W*/kg)	0.76	0.92	0.31	0.35	0.37
			SAR decrease between the top and bottom positions		
Frequency (MHz)	859	925	1795	1920	2045
1-g SAR (*W*/kg)	1.00 (−2.81 dB)	0.87 (−2.29 dB)	1.14 (−4.26 dB)	1.08 (−4.67 dB)	0.96 (−3.68 dB)
10-g SAR (*W*/kg)	0.66 (−2.71 dB)	0.52 (−1.95 dB)	0.56 (−4.48 dB)	0.49 (−3.80 dB)	0.39 (−3.13 dB)

REFERENCES

1. K.L. Wong and C.H. Huang, Bandwidth-enhanced PIFA with a coupling feed for quad-band operation in the mobile phone, Microwave Opt Technol Lett 50 (2008), 683–687.
2. K.L. Wong and C.H. Huang, Compact multiband PIFA with a coupling feed for internal mobile phone antenna, Microwave Opt Technol Lett 50 (2008), 2487–2491.
3. J. Ollikainen and A. Lehtola, Internal multi-band antenna with improved radiation efficiency, U.S. Patent No. 6,552,686 B2, 2003.
4. Y.X. Guo, M.Y.W. Chia, and Z.N. Chen, Miniature built-in multiband antennas for mobile handsets, IEEE Trans Antenn Propag 52 (2004), 1936–1944.
5. K.L. Wong, L.C. Chou, and C.M. Su, Dual-band flat-plate antenna with a shorted parasitic element for laptop applications, IEEE Trans Antenn Propag 53 (2005), 539–544.
6. K.L. Wong and Y.C. Lin, Thin internal planar antenna for GSM/DCS/PCS/UMTS operation in a PDA phone, Microwave Opt Technol Lett 47 (2005), 429–432.
7. J. Ollikainen, O. Kivekas, C. Ichein, and P. Vainikainen, Internal multiband handset antenna realized with an integrated matching circuit, Proceedings of the 12th International Conference Antennas Propagation, Vol. 2, 2003, pp. 629–632.
8. M. Tzortzakakis and R.J. Langley, Quad-band internal mobile phone antenna, IEEE Trans Antenn Propag 55 (2007), 2097–2103.
9. J. Villanen, C. Icheln, and P. Vainikainen, A coupling element-based quad-band antenna element structure for mobile terminals, Microwave Opt Technol Lett 49 (2007), 1277–1282.
10. T. Oshiyama, H. Mizuno, and Y. Suzuki, Multi-band antenna, U.S. Pat. Publ. No. 2007/0249313, 2007.
11. K.L. Wong, Planar antennas for wireless communications, Wiley, New York, 2003.
12. K.L. Wong and C.H. Chang, WLAN chip antenna mountable above the system ground plane of a mobile device, IEEE Trans Antenn Propag 53 (2005), 3496–3499.
13. K.L. Wong and C.H. Chang, Surface-mountable EMC monopole chip antenna for WLAN operation, IEEE Trans Antenn Propag 54 (2006), 1100–1104.
14. K.L. Wong, Y.C. Lin, and B. Chen, Internal patch antenna with a thin air-layer substrate for GSM/DCS operation in a PDA phone, IEEE Trans Antenn Propag 55 (2007), 1165–1172.
15. K.L. Wong, Y.C. Lin, and T.C. Tseng, Thin internal GSM/DCS patch antenna for a portable mobile terminal, IEEE Trans Antenn Propag 54 (2006), 238–242.
16. Y.W. Chi and K.L. Wong, Internal compact dual-band printed loop antenna for mobile phone application, IEEE Trans Antenn Propag 55 (2007), 1457–1462.
17. Y.L. Kuo and K.L. Wong, Printed double-T monopole antenna for 2.4/5.2 GHz dual-band WLAN operations, IEEE Trans Antenn Propag 51 (2003), 2187–2192.
18. Ansoft Corporation HFSS, Available at: http://www.ansoft.com/products/hf/hfss/.
19. SEMCAD, Schmid & Partner Engineering AG (SPEAG), Available at: http://www.semcad.com.
20. C.I. Lin and K.L. Wong, Printed monopole slot antenna for internal multiband mobile phone antenna, IEEE Trans Antenn Propag 55 (2007), 3690-3697.
21. P. Vainikainen, J. Ollikainen, O. Kivekas, and I. Kelander, Resonator-based analysis of the combination of mobile handset antenna and chassis, IEEE Trans Antenn Propag 50 (2002), 1433–1444.

DUAL-BACKLIGHT UNIT BASED ON A SINGLE LIGHT SOURCE INTEGRATED WITH A BEAM SPLITTING REFLECTOR

Chan-Kyu Park, Hak-Soon Lee, and Sang-Shin Lee
Department of Electronic Engineering, Kwangwoon University, 447-1 Wolgye-Dong, Nowon-Gu, Seoul 139-701, Republic of Korea; Corresponding author: slee@kw.ac.kr

Received 20 August 2008

ABSTRACT: *A dual-backlight unit incorporating a single light source integrated with a beam splitting reflector was demonstrated, providing a surface light beam for both the keypad and display section simultaneously. The reflector was realized by aligning a groove substrate with a matching cover, and a light guiding module comprising a stack of light guide panels and prism/diffuser sheets was attached to both sides of the reflector. A light emanating from the light source—placed in the middle of the substrate—undergoes a series of reflections through the reflector to reach the input of the light guiding module. Then it is transformed into a surface light beam, which is used to irradiate the keypad and display sections. As for the accomplished dual-backlight unit, the measured average luminance and the spatial luminance uniformity were respectively about 420 cd/m^2 and 70% for the keypad section, and 640 cd/m^2 and 80% for the display section.* © 2009 Wiley Periodicals, Inc. Microwave Opt Technol Lett 51: 1257–1260, 2009; Published online in Wiley InterScience (www.interscience.wiley.com). DOI 10.1002/mop.24297

Key words: *dual backlight; LED; beam splitter; illumination design*

1. INTRODUCTION

The mobile handset has witnessed immensely growing demand as a result of the advent of various wireless communication services. A light emitting diode (LED) was widely accepted as a prominent light source for the implementation of a backlight unit (BLU), which plays the role of illuminating the keypad and/or the display section of mobile handsets or other digital devices like monitors [1, 2]. To realize a cost effective BLU relying on LEDs, it is essential to lower the electrical power consumption and to simplify the